GRAPHICAL MODELS AND IMAGE PROCESSING
Vol. 57, No. 3, May, pp. 197–205, 1995

Entropic Thresholding Using a Block Source Model

AZEDDINE BEGHDADI

Laboratoire des Propriétés Mécaniques et Thermodynamiques des Matériaux CNRS LP 9001, Université Paris Nord, Avenue Jean Baptiste Clément, 93 430 Villetaneuse, France

ALAIN LE NÉGRATE

Laboratoire d'Ethologie Expérimentale et Comparée, URA 667, Université Paris Nord, Avenue Jean Baptiste Clément, 93 430 Villetaneuse, France

AND

PATRICK VIARIS DE LESEGNO

Laboratoire des Propriétés Mécaniques et Thermodynamiques des Matériaux CNRS LP 9001, Université Paris Nord, Avenue Jean Baptiste Clément, 93 430 Villetaneuse, France

Received April 5, 1993; revised January 9, 1995; accepted February 8, 1995

Since the pioneer work of Frieden (*J. Opt. Soc. Am.* 62, 1972, 511–518; *Comput. Graphics Image Process.* 12, 1980, 40–59), the entropy concept is increasingly used in image analysis, especially in image reconstruction, image segmentation, and image compression. In the present paper a new entropic thresholding method based on a block source model is presented. This new approach is based on a distribution-free local analysis of the image and does not use higher order entropy. Our method is compared to the existing entropic thresholding methods. © 1995 Academic Press, Inc.

1. INTRODUCTION

The idea of using the entropy concept in communication systems has become more appealing since the excellent work of Shannon [1]. In image analysis problems this universal concept [2] has been an attractive and powerful tool in image restoration and image segmentation, since the pioneer work of Frieden [3, 4] and Jaynes [5].

In restoration problems the basic idea consists in defining a statistical model for the image and then an entropy which is maximized, under some constraints, in order to get an image which fits the incomplete known data. This approach used by Skilling *et al.* [6–8] and Djafari [9] is called the MAXENT method or maximum entropy method.

In image segmentation the use of the entropy concept has been introduced, for the first time, by Pun [10, 11] for gray-level thresholding. Since then, Johannsen and Bille [12], Kapur *et al.* [13], Sahoo and Wong [14, 15], Abutaleb [16] and Pal and Pal [17, 18] have continued this work.

For many important applications in biomedical image analysis [19] or industrial inspection, the need to design a decision function allowing the discrimination of objects in a given scene often arises. Given the diversity in gray-level thresholding techniques [14, 20], the natural question is: How do the techniques compare, and which is the best?

The intent of this paper is not to answer this question but to propose a new approach of gray-level thresholding based on the digital entropy concept already used by Pun. In Pun's method, the a posteriori entropy of the gray-level histogram is maximized to get the optimum gray-level threshold. However, this approach presents some drawbacks that have been pointed out by Kapur *et al.* [13] who proposed another algorithm to correct the errors introduced in the first method of Pun [10]. Note that the method of Kapur *et al.* is very similar to that developed by Johannsen and Bille [12]. Both methods use the first-order entropy. However, though Kapur *et al.*'s algorithm has given some improvements to Pun's method, some questions still are unsolved as have been already noted by Pun. Indeed, an open question is: What happens if two different images have the same histogram? This leads to a second question: Will it be necessary to use higher order entropy?

These two questions induced Pal and Pal [17, 18] to use the probability of co-occurrence of the gray levels to define the entropy. Then, they introduced higher order entropy for gray-level thresholding. Their algorithm is based on a second-order statistic analysis already developed in a previous paper by Deravi and Pal [21].

1077-3169/95 $6.00

In the same time Abutaleb [16] proposed a very similar approach using a two-dimensional entropy for gray-level thresholding. His method is also based on a local analysis of the image. A 2D histogram is computed by examining the image through 3×3 overlapping neighborhoods. In each 3×3 neighborhood the mean gray level is computed and associated to the gray level of the central pixel to form the corresponding entry in the 2D histogram representing the probability of co-occurrence of the pair (gray level, mean gray level). Abutaleb has compared his algorithm to that of Pun and Kapur and has shown its efficiency in the threshold detection accuracy. But his algorithm requires an increased computational time, since the entropy criterion function is bidimensional. Furthermore, in Abutaleb's method two thresholds are computed but Abutaleb did not explicitly say how to threshold the image with respect to the bidimensional function. In fact, the two gray-level thresholds which maximize the decision function define four regions in the (gray level, mean gray-level) space. But, only two quadrants, namely the object and the background quadrants, are considered in the computation. The two others which contain information about object/background transitions and noise are ignored in the method of Abutaleb. This drawback has been noted by Brink [22] who proposed an improvement of the method by using the max–min technique to detect the optimum threshold. However, this method is much time consuming since it searches the gray-level threshold in a 4D space. In contrast, in Pal and Pal's method one optimum gray-level threshold is computed from a second-order entropy and the method is faster than that of Abutaleb. Furthermore, in the method of Pal and Pal object/background and background/object transitions are taken into account. Indeed, for a gray-level threshold t the co-occurrence matrix $[C]$, where C_{ij} is the number of occurrences of pairs of pixels, that with i gray-level and the neighbor (the upper or the left one) with j gray-level, is subdivided into four quadrants A, B, C, and D representing respectively object ($i \leq t, j \leq t$), object/background transition ($i \leq t, j > t$), background ($i > t, j > t$), and background/object transition ($i > t, j \leq t$). Pal and Pal define two entropies, namely the local entropy H_{AC} corresponding to the case when the image is viewed as composed of two classes, object and background; and the conditional entropy H_{BD} when only transition regions B and D are considered. Thus, two algorithms are proposed. The first one uses a second-order local entropy H_{AC} and the second is based on the conditional entropy H_{BD}. Both entropies are computed from the probability of co-occurence of gray-level pairs in a 2×2 neighborhood.

In our approach we show that it is possible to exploit the spatial correlations of the pixels without using higher order entropy as in Pal and Pal's and Abutaleb's methods. The basic idea of our method is to define another symbol source in the image which leads to a first-order entropy nonsensitive to the gray-level distribution in contrast to the methods of Pun, to that of Bille and Johannsen, and to that of Kapur *et al.*

Following the idea of Kunt developed in his strategy of coding facsimile images [23], a new source model for entropic thresholding is derived and evaluated through a comparison with the existing entropic methods.

The organization of the paper is as follows. The new source model for entropic thresholding is presented in Section 2. In this section we describe and discuss two approaches. In Section 3, we present the results obtained on some images. Finally, in Section 4 the overall valuations are summarized and discussed.

2. A NEW SOURCE MODEL FOR ENTROPIC THRESHOLDING

Before introducing the block source model, let us recall some definitions and statements derived from the information theory [2] and used in this paper. To measure the entropy associated with a given experiment one has to define the corresponding source of information and a set of associated symbols. It becomes then possible to define a random variable x, which takes its values in the set of the possible symbols, and consequently a probability function $P(x)$. For example, in the case of a digital image the elementary source is the pixel and the associated symbols could be the gray-level values. In this case the probability P_k that a pixel (i, j) randomly selected from the digital image will have some gray-level could be approximated by the relative frequency (N_k/N) at which this gray level occurs in the digital image of size N. If we have some prior measure m_k about the state k one could use the Shannon–Jaynes entropy or the Kullback–Leibler number [24], which was extensively used in image restoration methods [6–8] and defined by

$$H = -\sum_k P_k \log \frac{P_k}{m_k}. \tag{1}$$

It is a measure of the information content in the probability distribution P_k relative to the given prior m_k. If we have no prior knowledge, we take all m_k equal to a constant which yields to the well-known Shannon entropy defined by

$$H = -\sum_k P_k \log P_k. \tag{2}$$

In the following the entropy of Shannon given by Eq. (2) is used. In order to define a probability distribution and thus the associated entropy, the image is analyzed with

respect to a given source model. The basic idea of the proposed method is to analyze the image through a window which is considered as a source of symbols corresponding to the gray-level values of the pixels within it. That is, for each gray-level threshold candidate, the two-tone image composed of black and white pixels is analyzed through an elementary window which can have a fixed or a variable size. In the following sections we deal with the two cases and thus two approaches will be proposed. The symbols associated with this source are the black and white patterns observed through the analysis window.

The optimum level is the one which gives a compressed version of the original image containing the greatest amount of information associated with the given source symbol. Thus, the entropy takes its maximum value at a gray level at which one would expect the threshold value.

2.1. *First Approach—Fixed Block Method (FBM)*

Let A denote the grid of sample points of a picture of size $L \times M$, i.e., the set of points (i, j), where $i = 1, 2, \ldots, L$ and $j = 1, 2, \ldots, M$, and g_{ij} the gray level of the (i, j) pixel. For a gray-level threshold t the picture A can be viewed as a set of juxtaposed binary blocks of size $m \times n$ pixels where each pixel of an original gray-level g_{ij} is either black (if $g_{ij} \leq t$) or white (if $g_{ij} > t$). The source is then the block of size $m \times n$ and the 2^{mn} different binary pixel configurations of the block can be considered as source messages. For the sake of simplicity, we chose $m = n = s$, i.e., the image is subdivided into square blocks of the same size $\mathbf{K} = s \times s$. In this approach the blocks are assumed to be statistically independent. This assumption will be dropped out in the next approach.

Let $B = \{0, 1\}^{\mathbf{K}}$ denote the set of binary $(s \times s)$ blocks. The number of elements in B, i.e., the number of possible block configurations is $N = 2^{\mathbf{K}}$. Let B_k be a subset of $(s \times s)$ blocks containing k ones (white pixels) and $\mathbf{K}$-k zeros (black pixels). The binary source probabilities $\{P_k\}$, $P_k = \text{Prob}\{\text{block} \in B_k\}$ is measured by analyzing all juxtaposed blocks in the image. An example of the possible pixel configurations or symbols corresponding to $s = 2$ and $k = 2$ is given in Fig. 1.

In this approach there are three major constraints. The first one is the large number of different configurations when s is large. For instance, a block size of 5×5 pixels requires an array of 2^{25} entries to store the number of different configurations. The different configurations could be stored in a K-bits register. The second constraint is the choice of the block size. Indeed, a small size for the analysis block could not be sufficient to describe the geometric content of the image. The last constraint is due to the fact that in this approach the blocks are assumed statistically independent. But this restriction is counterbalanced by the great number of possible symbols associated with the pixel configurations of the analysis block.

FIG. 1. Example of the possible symbols associated with a block source for $s = 2$ and $k = 2$.

Once the probability distribution is computed, one can determine the optimum gray-level threshold by maximizing the associated entropy. The search procedure consists in varying t and searching for the maximum value of the a posteriori entropy $H(t)$ given below:

$$H(t) = -\sum_{k=1}^{N} P_k(t) \log P_k(t). \tag{3}$$

Here P_k is the probability to find a block in the kth configuration. Then, the optimum threshold t^* is $t^* = \text{Arg}\{\text{Max}[H(t)], t \in [g_{\min}, g_{\max}]\}$, where $[g_{\min}, g_{\max}]$ is the gray-level range. It can be easily shown that $H(t)$ is bounded by the maximum value $H_{\max}(t) = \log_2 K$, which corresponds to a uniform probability distribution, i.e., $P_k(t) = 1/2^K$. This corresponds to a purely random image or a white noise image.

2.2. *Second Approach—Moving Block Method (MBM)*

In the previous approach, the image was subdivided into juxtaposed blocks. Now a moving window with a variable size is used to analyze the image. In order to use large sizes for the analysis window, the block configurations are assumed to be indistinguishable. That is, for a given block size and a candidate threshold t different configurations of blocks containing the same number of white pixels are considered as the occurrence of the same source symbol. For example, for $s = 2$ and $k = 2$, the six configurations shown in Fig. 1 are equivalent. For a threshold candidate t the number $N_k(s, t)$, representing the number of blocks containing k white pixels, whatever the spatial organization of the pixels in the block, is computed. Then the a posteriori probability $P_k(s, t)$ that a block of size $s \times s$ randomly selected from the digital image will have N_k white pixels could be approximated by the relative frequency $(N_k(s, t)/N_s)$ at which this configuration occurs in the digital image of size N_s blocks. Obviously the number of possible configurations is $s^2 + 1$ if the configuration corresponding to a totally black block (i.e., $k = 0, 1, \ldots, s^2$) is taken into account. Therefore,

the maximum a posteriori entropy which corresponds to an uniform probability is

$$H_{\max}(s, t) = \log(s^2 + 1), \tag{4}$$

and the a posteriori entropy associated with the probability distribution $P_k(s, t)$ is

$$H(s, t) = -\sum_{k=0}^{s^2} P_k(s, t) \log P_k(s, t). \tag{5}$$

Block Size Effect. Note that for $s = 1$, the proposed algorithm yields a trivial threshold which splits the gray-level histogram into two equal populations as in the first approach of Pun [10]. Taking into account this drawback, the block size must be greater than one pixel. Furthermore, if $s = 1$, we do not exploit the spatial correlation of the pixels, whereas the aim of the proposed approach is to exploit these correlations.

In the other extreme case, i.e., $n = L$, $m = M$, when the whole image is considered as a unique block, the entropy is zero. Indeed, the degree of uncertainty is zero since there is one possible configuration. Between these two extreme situations one has to adapt the block size to the image structure as in the coding technique of Kunt [23]. For structured images the block size must be small enough and comparable to that of the likely pattern in the image, whereas for unstructured images the block size can be larger.

The Optimum Block Size. Note that at small s the local patterns are simple. But they are highly correlated with each other. The one-cell function $P_k(s, t)$ at small s does not contain these correlations. At large s the local patterns are statistically uncorrelated but each one of them is nearly as complex as the geometry of the whole two-tone image. There must then exist an intermediate length scale s^* at which on the one hand the local geometries are relatively simple, and on the other hand the single-block distribution function has sufficient nontrivial geometric content to be a good first approximation of the geometrical information. The idea is then to maximize the geometrical content contained in $P_k(s, t)$ with respect to s and t. This can be achieved by using the maximum entropy principle.

It is possible to overcome the ambiguity in the choice of the block size. Indeed, the entropy maximization can be performed in the 2D space (s, t), representing the gray-level threshold t and the block size s. As in Abutaleb's approach, if for a given application an accuracy in the threshold detection is required, one can maximize the criterion entropy $H(s, t)$ with respect to the gray-level threshold t and to the block size s. This procedure is of course time consuming but some improvements can be done to localize the entropy maximum. For example, one can restrict the domain of investigation by examining some relevant quantities in the image such as the gray-level histogram [25, 26]. Since the entropy depends on the considered block size, one has to normalize the entropy in order to compare the values obtained for the different block sizes. Then, the a posteriori configuration entropy reads

$$H^*(s, t) = H(s, t)/H_{\max}(s, t). \tag{6}$$

Now the configuration entropy is such that $0 \leq H^*(s, t) \leq 1$, for all s values.

To get the optimum gray-level threshold we proceed by increasing t and s successively. As in the first approach, the optimum threshold is obtained by maximizing the a posteriori configuration entropy,

$$t^* = \text{Arg}\{\text{Max}[H^*(s, t); t \in [t_{\min}, t_{\max}]; s = 2, \ldots, s_c]\}, \tag{7}$$

where $[t_{\min}, t_{\max}]$ is the domain of investigation for the candidate threshold and s_c is the maximum block size which is taken to be equal to $L/2$.

3. RESULTS AND DISCUSSION

Many methods for image segmentation have been developed. However, little effort has been spent on the development of a quantitative and objective study on the validation of these methods [27]. This is due to the fact that the selection of an appropriate technique for a specific type of image is a difficult problem. As a consequence no single standard method of image segmentation has emerged and all the existing methods are very often ad hoc [28–30]. The same conclusion appears in a recent review of image segmentation methods [31]. Recently, Zhang and Gerbrands [32, 33] have proposed a quantitative and objective approach for image segmentation evaluation and comparison. The basic idea is similar to that of Yasnoff *et al.* [34]. It consists in defining quantitative error measures useful in the comparison of image segmentation techniques. Five properties which must be verified by such measures have been defined. The error measures used by Zhang and Gerbrands are similar to the misclassification error computed from the standard confusion matrix defined in [34]. The same idea has been also used by Lee *et al.* for a comparison study of some global thresholding methods [35].

The proposed method has been tested on synthetic and actual images and has been compared to the existing entropic thresholding methods. The obtained results are discussed below. For actual images only subjective crite-

ria, namely, the visual perception quality, are used to compare the results obtained by the different entropic methods. The synthetic image is used for a quantitative and objective comparison of the discussed methods.

Remark. Note that the first approach is faster than the second one since the entropy maximum searching requires only one block size. Furthermore, a small block size is sufficient to take into account a large number of configurations compared to the second method. However, the block are assumed statistically independent, whereas in the second approach the block dependence is taken into account since the analysis window is moving. Also note that the proposed method is noise sensitive. Thus, a filtering process is often necessary before thresholding the image.

3.1. *A Qualitative and Subjective Evaluation of the Proposed Method*

The image shown in Fig. 2a is a digitized transmission electron micrograph of a gold thin film. The light background is the glass onto which gold is deposited by coevaporation. The gold clusters appear in dark tone. We know that this physical image is composed of two classes of pixels: gold pixels and glass pixels. The algorithm of Abutaleb totally fails for this image as shown in Fig. 2b. Note that Abutaleb did not tell how to threshold a given image. Through his results, it seems that he used one threshold and consequently the pixels corresponding to object/background and background/object transitions are neglected. In the present study, these transitions are taken into account, thus two thresholds corresponding to the maximum of the two-dimensional criterion function of Abutaleb are computed. Then four regions are defined in the decision space. For this particular image, only two regions were detected in the decision space.

Through Figs. 2b–2h, one can observe that the results obtained with our method (the MBM algorithm, Fig. 2c and the FBM algorithm, Fig. 2d), the method of Pun (Fig. 2e), the method of Kapur *et al.* (Fig. 2f) and algorithm 2 of Pal and Pal (Fig. 2h) are identical. But algorithm 1 of Pal and Pal (Fig. 2g) totally fails for this image.

Figure 3a shows another actual image representing a material plastically deformed in fatigue and observed in the electron microscope. One can see a dark background, light bands, and a light grid. We tested the entropic thresholding algorithms mentioned above on this image. The obtained results shown in Figs. 3b to 3h clearly demonstrate the superiority of our method (MBM, Fig. 3c and FBM, Fig. 3d) and those of Pun (Fig. 3e) and Kapur *et al.* (Fig. 3f) for this particular example. In fact, the grid is totally eliminated by all the other algorithms using a second-order entropy, whereas it is preserved by our algorithm and those of Kapur *et al.* and Pun.

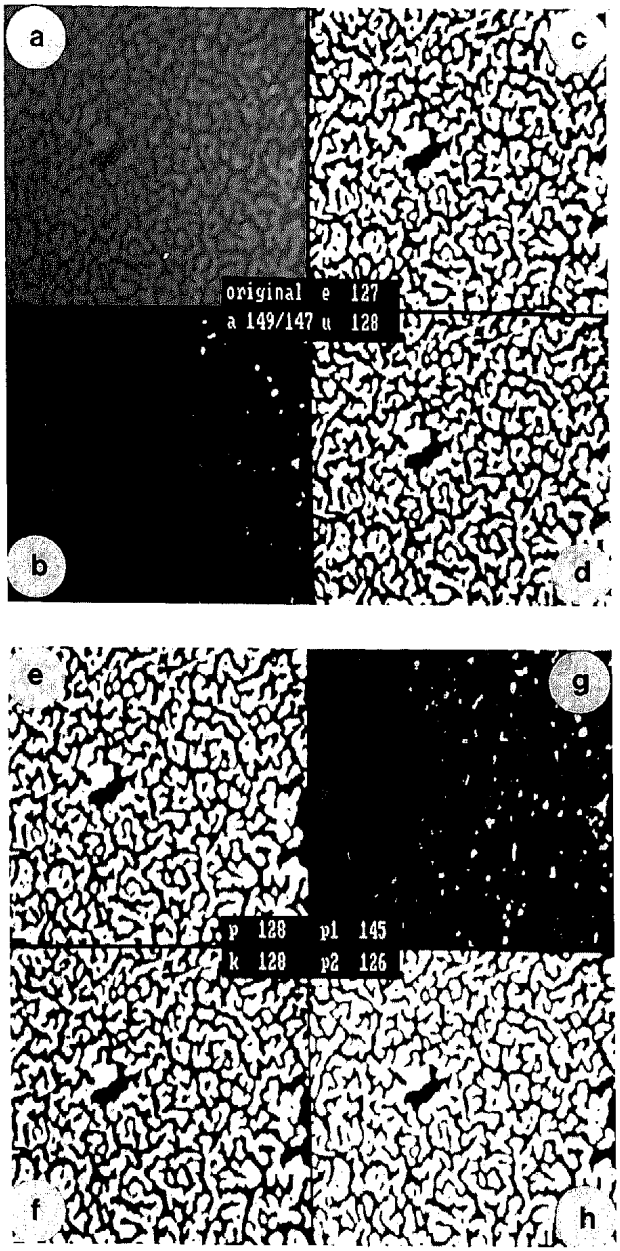

FIG. 2. (a) Original image, (b) algorithm of Abutaleb, (c) MBM algorithm, (d) FBM algorithm (e) method of Pun, (f) method of Kapur *et al.*, (g) algorithm 1 of Pal and Pal, and (h) algorithm 2 of Pal and Pal.

Another image representing a girl's portrait is used as a test image. In this case, our method is superior to all the other methods. In fact, even Kapur *et al.*'s method fails in preserving some details. For instance, the nose is well preserved with our algorithms (MBM, Fig. 4c and FBM, Fig. 4d), whereas with Kapur *et al.*'s method (Fig. 4f) and with Pun's (Fig. 4e) it is nearly suppressed. The same effect can be noted for the girl's glasses. The other methods of Abutaleb (Fig. 4b) and Pal and Pal (Figs. 4g and 4h) totally fail for this special case.

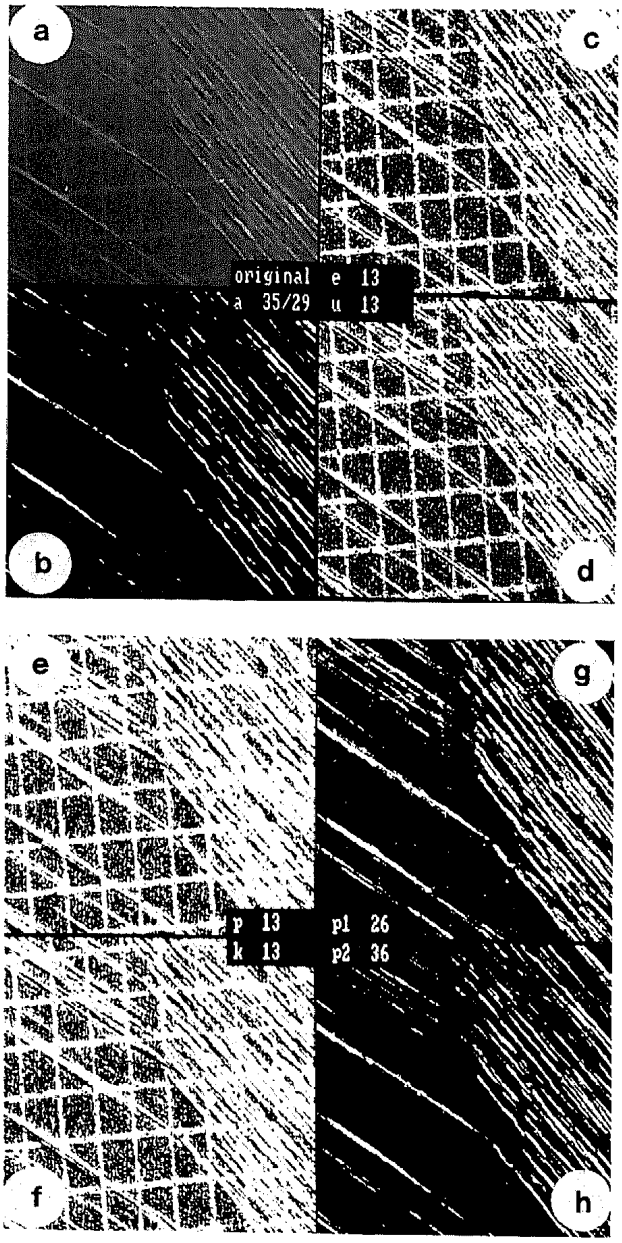

FIG. 3. (a) Original image, (b) algorithm of Abutaleb, (c) MBM algorithm, (d) FBM algorithm (e) method of Pun, (f) method of Kapur *et al.*, (g) algorithm 1 of Pal and Pal, and (h) algorithm 2 of Pal and Pal.

FIG. 4. (a) Original image, (b) algorithm of Abutaleb, (c) MBM algorithm, (d) FBM algorithm, (e) method of Pun, (f) method of Kapur *et al.*, (g) algorithm 1 of Pal and Pal, and (h) algorithm 2 of Pal and Pal.

Another interesting result is that our approach yields a threshold between the two extreme values, confirming thus that our method is a compromise between the global approaches of Pun and Kapur *et al.* and the local approaches of Abutaleb and Pal and Pal.

3.2. *A Quantitative and Objective Comparison*

In order to compare the discussed methods we use the same approach of Zhang and Gerbrands inspired from that of Yasnoff *et al.* Synthetic images are then used for quantitative evaluation of our method and for comparison. The first synthetic image is generated by the luminance function

$$g(x, y) = g_0 + g_m \cos 2\pi\nu x, \tag{8}$$

where (x, y) are the pixel coordinates, g_0 is the mean gray-level of the background, g_m is the AC component, and ν is the spatial frequency. One can generate different shapes by varying the spatial frequency and the global contrast given by $C = g_m/g_0$. The $g(x, y)$ is nothing else than a sinusoidal grid pattern. Figure 5a depicts the half period, say $a = 1/2\nu$, of this signal, for a given y value and the corresponding gray-level histogram $P(g)$. Here,

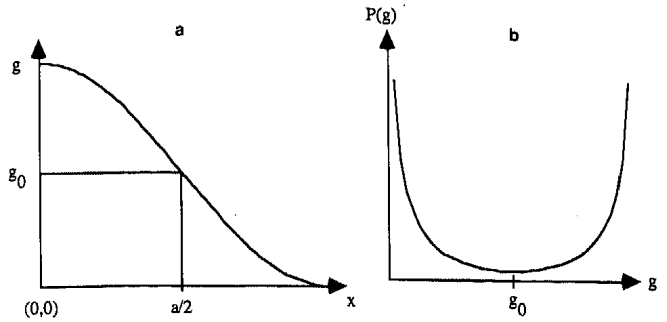

FIG. 5. (a) Luminance profile and (b) histogram of the computer-generated image.

the gray-level threshold is the level of points lying on the edge. It can be easily computed by detecting the zero-crossing of the second derivative of $g(x, y)$ function. Indeed, the equation $\nabla^2 g$ to zero yields $x = a/2$ which corresponds to the threshold $t^* = g(a/2) = g_0$. This result can be also obtained by analyzing the luminance distribution function $P(g)$. In fact, it can be easily shown that

$$P(g) = \frac{1}{2\pi\nu g_m} \frac{1}{\sqrt{1 - ((g - g_0)/g_m)^2}}. \tag{9}$$

The representative curve shown in Fig. 5b clearly depicts a deep valley where the optimum threshold can be obtained by solving the equation $dP/dg = 0$, which leads to $g = g_0$. A half period of this synthetic image has been generated with $g_0 = 64$ and a maximum contrast $C = 1$. The optimum threshold is equal to $g_0 = 64$ as demonstrated previously. All the discussed thresholding algorithms have been applied to this image. The obtained results are in good agreement with the theoretical prevision except for the algorithm of Pal and Pal based on the conditional entropy. To show why this algorithm totally fails for this image let us consider an 8×8 matrix $[g]$ representing a half period of signal $g(x, y)$ generated with $a = 8$, $g_0 = 4$, $C = 1$, and $0 \le x, y < 8$:

$$[g] = \begin{bmatrix} 8 & 7 & 6 & 5 & 3 & 2 & 1 & 0 \\ 8 & 7 & 6 & 5 & 3 & 2 & 1 & 0 \\ 8 & 7 & 6 & 5 & 3 & 2 & 1 & 0 \\ 8 & 7 & 6 & 5 & 3 & 2 & 1 & 0 \\ 8 & 7 & 6 & 5 & 3 & 2 & 1 & 0 \\ 8 & 7 & 6 & 5 & 3 & 2 & 1 & 0 \\ 8 & 7 & 6 & 5 & 3 & 2 & 1 & 0 \\ 8 & 7 & 6 & 5 & 3 & 2 & 1 & 0 \end{bmatrix}$$

The edge gray-level or the threshold is obviously equal to 4 in this case. The corresponding co-occurrence matrix of $[g]$, computed for a distance equal to 1, in both horizontal and vertical directions as in [17, 18],

$$[C] = \begin{bmatrix} 7 & 0 & 0 & 0 & 0 & 0 & 0 & 0 & 0 \\ 8 & 7 & 0 & 0 & 0 & 0 & 0 & 0 & 0 \\ 0 & 8 & 7 & 0 & 0 & 0 & 0 & 0 & 0 \\ 0 & 0 & 8 & 7 & 0 & 0 & 0 & 0 & 0 \\ 0 & 0 & 0 & 0 & 0 & 0 & 0 & 0 & 0 \\ 0 & 0 & 0 & 8 & 0 & 7 & 0 & 0 & 0 \\ 0 & 0 & 0 & 0 & 0 & 8 & 7 & 0 & 0 \\ 0 & 0 & 0 & 0 & 0 & 0 & 8 & 7 & 0 \\ 0 & 0 & 0 & 0 & 0 & 0 & 0 & 8 & 7 \end{bmatrix}.$$

Now, Pal and Pal's second algorithm relies on the conditional entropy to compute the threshold which in this case is equal to 0 for all possible threshold gray-levels. Indeed, one can notice from this co-occurrence matrix that the two conditional entropies corresponding respectively to object/background and background/object transitions are equal to 0 for all gray-level thresholds. That means that the second algorithm of Pal and Pal gives a threshold equal to 0, while the optimum threshold is equal to 4 in this case, as analytically shown before. This example shows that the Pal and Pal's second algorithm is not always superior to the first one as claimed by them in [17, 18].

Now if a complete period of the signal $g(x, y)$ is used, all the discussed algorithms give a threshold value which deviates from the optimum value except for the first algorithm of Pal and Pal and our two algorithms. The deviation of the other algorithms from the exact threshold value ($t^* = 64$) is about two or three levels. Furthermore, the second algorithm of Pal and Pal totally fails.

Another synthetic image similar to that used in [32, 33] is used to evaluate the proposed methods and to compare them to the other entropic methods. Figure 6 depicts the results obtained when applying the different algorithms to the blurred image (Fig. 6b) obtained by convolving the original image (Fig. 6a) with a Gaussian filter with a standard deviation $\sigma = 5$. This synthetic image of size 128×128 is composed of a background of gray-level-64, four disks (radius 15 pixels) with a homogeneous gray-level 127 and one circular disk (radius 31 pixels) with the same gray-level 127. Note that all the cited algorithms give the exact threshold ($t^* = 64$), except for the second algorithm of Pal and Pal. This is not surprising since this algorithm uses the background/object transition information. Indeed, this image does not contain transition regions.

Note that in [32, 33] the quantitative measure for comparison is not directly computed from the thresholded

image but after applying a morphological filter to the segmented image. Thus, some misclassified pixels corresponding essentially to the synthetic additive noise are smoothed out by morphological filter, namely an opening or a closing [36]. In the present study we do not modify the obtained segmented image as done in [33]. Furthermore, the approach of Zhang and Gerbrands, which consists of defining the optimum gray level as the level which preserves some morphological parameters such as the area or the perimeter of the objects after applying a degradation process to the image, is not appealing. Indeed, it is well known that applying a blurring function to a given image increases the object size and consequently shifts the edge location [37]. Thus, using morphological parameter preservation as criterion for performance assessment is not relevant. Then in the present approach we use the measure of the blurring effect as a quantitative measure for comparison of the different algorithms.

The obtained results shown in Fig. 6 confirm once again the superiority of the proposed methods, especially the MBM algorithm, over the other existing entropic thresholding methods. Indeed, the thresholded image (Fig. 6i) points out the exact location of the edges corresponding to a Gaussian filter of a standard deviation $\sigma = 5$. This result is confirmed when applying a second-derivative operator such as the digital Laplacian. All the other methods give a gray-level threshold which does not correspond to the exact background/object transition location (see Figs. 6c–6h).

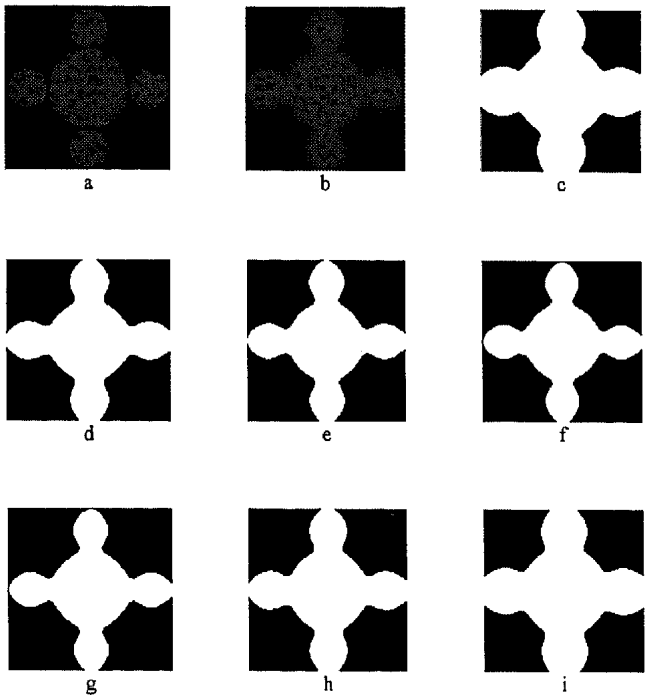

FIG. 6. Synthetically generated image: (a) original image, (b) blurred image, (c) algorithm of Kapur *et al.* ($t^* = 72$), (d) algorithm of Pun ($t^* = 90$), (e) algorithm of Abutaleb ($t^* = 96$), (f) algorithm 1 of Pal and Pal ($t^* = 99$), (g) algorithm 2 of Pal and Pal ($t^* = 99$), (h) FBM algorithm ($t^* = 90$), and (i) MBM algorithm ($t^* = 76$).

4. CONCLUSION

It is demonstrated through some examples that our gray-level thresholding method using a first-order entropy is superior to the existing entropic thresholding methods in some cases. It is also shown that for some images, the methods of Pal and Pal and that of Abutaleb are not superior to that of Kapur *et al.* as has been claimed by these authors in previous papers.

It is shown that the proposed method is a compromise between the global approaches of Pun, Johannsen and Bille, and Kapur *et al.* and the local approaches of Pal and Pal, and Abutaleb.

Through this paper, it is shown that it is possible to use a first-order entropy, which is gray-level histogram free, to localize the optimum gray-level threshold. Thus, we have given answers to Pun's questions. We have also shown that using a synthetic image where the gray-level threshold can be analytically computed is a good approach for comparing the image thresholding methods. This approach has been combined with that of Zhang and Gerbrands.

In this paper we have restricted our attention to one threshold, though the method can be extended to multithresholding cases which will be developed in the near future.

ACKNOWLEDGMENTS

The authors are grateful for the valuable comments of the reviewers which led to substantial improvements in the earlier version of the paper. One of the referees pointed out to us the useful results by Zhang and Gerbrands. A. Beghdadi thanks T. Huillet for fruitful discussion.

REFERENCES

1. C. E. Shannon, A mathematical theory of communications, *Bell. Syst. Tech. J.* **27**, 1948, 623–656.
2. L. Brillouin, *Science and Information Theory*, Academic Press, New York, 1956.
3. B. R. Frieden, Restoring with maximum likelihood and maximum entropy, *J. Opt. Soc. Am.* **62**, 1972, 511–518.
4. B. R. Frieden, Statistical models for the image restoration problem, *Comput. Graphics Image Process.* **12**, 1980, 40–59.
5. E. T. Jaynes, On the rationale of maximum entropy methods, *Proc. IEEE* **70**, 1982, 939–952.
6. J. Skilling and S. F. Gull, The entropy of an image, *SIAM Am. Math. Soc.* **14**, 1984, 167–187.
7. S. F. Gull and J. Skilling, Maximum entropy method in image processing, *IEEE Proc.* **134F**, 1984, 646–659.

8. S. F. Burch, S. F. Gull, and J. Skilling, Image restoration by a powerful maximum entropy method, *Comput. Vision Graphics Image Process.* **23,** 1983, 113–128.
9. A. Mohammad-Djafari and G. Demoment, Maximum entropy Fourier synthesis with application to diffraction tomography, *Appl. Opt.* **26,** 1987, 1745–1754.
10. T. Pun, A new method for gray-level picture thresholding using the entropy of the histogram, *Signal Process.* **2,** 1980, 223–237.
11. T. Pun, Entropic thresholding, a new approach, *Comput. Graphic Image Process.* **16,** 1981, 210–239.
12. G. Johannsen and J. Bille, A threshold selection method using information measure, in *Proceedings IEEE, 6th International Conference Pattern Recognition, Munich, Germany, 1982*, pp. 140–143.
13. J. N. Kapur, P. K. Sahoo, and A. K. C. Wong, A new method for gray-level picture thresholding using the entropy of the histogram, *Comput. Vision Graphics Image Process.* **29,** 1985, 273–285.
14. P. K. Sahoo, S. Soltani, and A. K. C. Wong, A survey of thresholding techniques, *Comput. Vision Graphics Image Process.* **41,** 1988, 233–260.
15. A. K. C. Wong and P. K. Sahoo, A gray-level thresholding selection method based on maximum entropy principle, *IEEE Trans. Syst. Man Cybernet.* **19**(4), 1989, 866–871.
16. S. A. Abutaleb, Automatic thresholding of gray-level pictures using two-dimensional entropy, *Comput. Vision Graphics Image Process.* **47,** 1989, 22–32.
17. N. R. Pal and S. K. Pal, Entropic thresholding, *Signal Process.* **16,** 1989, 97–108.
18. N. R. Pal and S. K. Pal, Entropy: A new definition and its applications, *IEEE Trans. Syst. Man Cybernet.* **21**(5), 1991, 1260–1270.
19. C. K. Chow and T. Kaneko, Automatic boundary detection of the left ventricule from cineangiograms, *Comput. Biombed. Res.* **5,** 1972, 388–410.
20. J. S. Weska, A survey of threshold selection techniques, *Comput. Graphics Image Process.* **7**(2), 1978, 259–265.
21. F. Deravi and S. K. Pal, Gray-level thresholding using second-order statistics, *Pattern Recognit. Lett.* **1,** 1983, 417–422.
22. A. D. Brink, Thresholding of digital images using two-dimensional entropies, *Pattern Recognit.* **25**(8), 1992, 803–808.
23. M. Kunt, Block coding of graphics: A tutorial review, *Proc. IEEE* **68**(7), 1980.
24. J. N. Kapur, Twenty-five years of maximum-entropy principle, *J. Math. Phys. Sci.* **17**(2), 1983, 103–156.
25. A. Rosenfeld and P. De La Torre, Histogram concavity analysis as an aid in threshold selection, Technical Report 1016, Computer Vision Laboratory, Computer Science Center, University of Maryland, College Park, Feb. 1981.
26. S. Boukharouba, J. M. Rebordao, and P. L. Wendel, An amplitude segmentation method based on the distribution function of an image, *Comput. Vision Graphics Image Process.* **29,** 1985, 47–59.
27. C. N. De Graaf, A. S. E. Koster, K. L. Vincken, and M. A. Viergever, Task-directed evaluation of image segmentation methods, in *Proceedings 11th International Conference on Pattern Recognition, The Hague, The Netherlands, 30 Aug.–3 Sept. 1993*, Vol. 3, pp. 219–222.
28. K. S. Fu and J. K. Mui, A survey on image segmentation, *Pattern Recognit.* **13,** 1981, 3–16.
29. A. Rosenfeld and A. Kak, *Digital Picture Processing*, 2nd ed., Academic Press, New York, 1982.
30. T. Pavlidis, *Structural Pattern Recognition*, Springer-Verlag, Berlin/New York, 1977.
31. N. R. Pal and S. K. Pal, A review on image segmentation techniques, *Pattern Recognit.* **26**(9), 1993, 1277–1294.
32. Y. J. Zhang and J. J. Gerbrands, Comparison of thresholding techniques using synthetic images and ultimate measurement accuracy, in *Proceedings 11th International Conference on Pattern Recognition, The Hague, The Netherlands, 30 Aug.–3 Sept. 1992*, Vol. 3, pp. 209–213.
33. Y. J. Zhang and J. J. Gerbrands, Objective and quantitative segmentation evaluation and comparison, *Signal Process.* **39,** 1994, 43–54.
34. W. A. Yasnoff, J. K. Mui, and J. W. Bacus, Error measures for scene segmentation, *Pattern Recognit.* **9,** 1977, 217–231.
35. S. U. Lee, S. L. Chung, and R. H. Park, A comparative performance study of several global thresholding techniques for segmentation, *Comput. Vision Graphics Image Process.* **52,** 1990, 171–190.
36. J. Serra, *Image Analysis and Mathematical Morphology*, Academic Press, London, 1982.
37. M. Shah and A. Sood, Pulse and staircase edge models, *Comput. Vision Graphics Image Process.* **34,** 1986, 321–343.